



Continuous  
measurements at the  
urban roadside in an  
ACSM

C. Sun et al.

This discussion paper is/has been under review for the journal Atmospheric Chemistry and Physics (ACP). Please refer to the corresponding final paper in ACP if available.

# Continuous measurements at the urban roadside in an Asian Megacity by Aerosol Chemical Speciation Monitor (ACSM): particulate matter characteristics during fall and winter seasons in Hong Kong

C. Sun<sup>1</sup>, B. P. Lee<sup>1</sup>, D. Huang<sup>2</sup>, Y. J. Li<sup>1,a</sup>, M. I. Schurman<sup>1</sup>, P. K. K. Louie<sup>3</sup>,  
C. Luk<sup>3</sup>, and C. K. Chan<sup>1,2</sup>

<sup>1</sup>Division of Environment, Hong Kong University of Science and Technology, Kowloon, Hong Kong, China

<sup>2</sup>Department of Chemical and Biomolecular Engineering, Hong Kong University of Science and Technology, Kowloon, Hong Kong, China

<sup>3</sup>Hong Kong Environmental Protection Department, Wan Chai, Hong Kong, China

<sup>a</sup>now at: School of Engineering and Applied Science, Harvard University, Cambridge, MA 02138, USA

Title Page

Abstract

Introduction

Conclusions

References

Tables

Figures



Back

Close

Full Screen / Esc

Printer-friendly Version

Interactive Discussion



Received: 2 June 2015 – Accepted: 12 June 2015 – Published: 16 July 2015

Correspondence to: C. K. Chan (keckchan@ust.hk)

Published by Copernicus Publications on behalf of the European Geosciences Union.

**ACPD**

15, 19405–19445, 2015

**Continuous  
measurements at the  
urban roadside in an  
ACSM**

C. Sun et al.

Title Page

Abstract

Introduction

Conclusions

References

Tables

Figures



Back

Close

Full Screen / Esc

Printer-friendly Version

Interactive Discussion



## Abstract

Non-refractory submicron aerosol is characterized using an Aerosol Chemical Speciation Monitor (ACSM) in the fall and winter seasons of 2013 at the roadside in an Asian megacity environment in Hong Kong. Organic aerosol (OA), characterized by application of Positive Matrix Factorization (PMF), and sulfate are found dominant. Traffic-related organic aerosol shows good correlation with other vehicle-related species, and cooking aerosol displays clear meal-time concentration maxima and association with surface winds from restaurant areas. Contributions of individual species and OA factors to high NR-PM<sub>1</sub> are analyzed for hourly data and daily data; while cooking emissions in OA contribute to high hourly concentrations, particularly during meal times, secondary organic aerosol components are responsible for episodic events and high day-to-day PM concentrations. Clean periods are either associated with precipitation, which reduces secondary OA with a lesser impact on primary organics, or clean oceanic air masses with reduced long-range transport and better dilution of local pollution. Haze events are connected with increases in contribution of secondary organic aerosol, from 30 to 50% among total non-refractory organics, and influence of continental air masses.

## 1 Introduction

The Special Administrative Region of Hong Kong (HKSAR) is a global logistics and finance center located at the south-eastern edge of the Pearl River Delta Region (PRD), China's largest manufacturing area and one of the world's most densely populated regions. Hong Kong has been plagued by deteriorating air quality, attributed to local emissions from traffic, residential and commercial activity, regional pollution from the PRD and long-range transport (Nie et al., 2013; Wong et al., 2013; Yuan et al., 2013).

High-time-resolution online instruments can characterize ambient aerosols quickly and mitigate the influence of changing environmental conditions. Few real-time studies

ACPD

15, 19405–19445, 2015

### Continuous measurements at the urban roadside in an ACSM

C. Sun et al.

Title Page

Abstract

Introduction

Conclusions

References

Tables

Figures

◀

▶

◀

▶

Back

Close

Full Screen / Esc

Printer-friendly Version

Interactive Discussion



## Continuous measurements at the urban roadside in an ACSM

C. Sun et al.

Title Page

Abstract

Introduction

Conclusions

References

Tables

Figures

◀

▶

◀

▶

Back

Close

Full Screen / Esc

Printer-friendly Version

Interactive Discussion



have been conducted in Hong Kong aside from recent measurement campaigns conducted by high resolution aerosol mass spectrometer (HR-AMS) (Lee et al., 2013; Li et al., 2013, 2015; Huang et al., 2015). Long-term AMS studies tend to be costly and time-consuming due to the complexity of the instrument. The ACSM, whose design is based on the AMS but has been substantially simplified, has seen a growing trend of use due to its comparative ease of operation, robustness, and sufficient time resolution (~ 20–60 min) for studies spanning months or longer. (Ng et al., 2011; Sun et al., 2012, 2013a, b; Budisulistiorini et al., 2013; Canonaco et al., 2013; Takahama et al., 2013; Bougiatioti et al., 2014; Petit et al., 2015; Ripoll et al., 2015; Tiitta et al., 2014; Minguillón et al., 2015).

This study presents the first ACSM characterization of particulate matter at a busy urban roadside station in Hong Kong with heavy traffic and commercial and residential activities. It aims to provide long-term characterization of particulate matter sources in a typical inner-city environment, enabling the identification of the relative importance of different sources and typical recurring patterns.

## 2 Experimental

The roadside measurement data were collected from 3 September to 31 December 2013 in Mong Kok (MK), an urban area with dense buildings and population in the Kowloon peninsula as part of a Hong Kong Environmental Protection Department (HKEPD) project (ref.: 13-00986). The sampling site was next to the road-side air quality monitoring station (AQMS) of HKEPD at the junction of the heavily trafficked Nathan Road and Lai Chi Kok Road (22°19'2" N, 114°10'06" E). The distribution of businesses in the vicinity varies, with restaurants mainly to the east, commercial buildings to the south and east, small shops for interior decoration, furniture and electrical goods to the west and residential buildings to the north of the sampling location (Lee et al., 2015). The sampling setup is described in detail in the Supplement, Sect. 1.

---

**Continuous  
measurements at the  
urban roadside in an  
ACSM**C. Sun et al.

---

[Title Page](#)[Abstract](#)[Introduction](#)[Conclusions](#)[References](#)[Tables](#)[Figures](#)[◀](#)[▶](#)[◀](#)[▶](#)[Back](#)[Close](#)[Full Screen / Esc](#)[Printer-friendly Version](#)[Interactive Discussion](#)

Non-refractory PM<sub>1</sub> (NR-PM<sub>1</sub>) species (sulfate, nitrate, ammonium, chloride, and organics) were measured in-situ by an Aerodyne Aerosol Chemical Speciation Monitor (ACSM, SN: 140–154). Other data including meteorological data (wind, temperature, relative humidity, solar irradiation), volatile organic compounds (VOCs) measured by an online gas-chromatography system (GC955-611 and GC955-811, Synspec BV), and standard criteria pollutants (NO<sub>x</sub>, SO<sub>2</sub> and PM<sub>2.5</sub>) were provided by the HKEPD, with equipment details available from the HKEPD air quality reports (Environmental Protection Department, 2013).

The acquired 20 min-average data were treated according to the general ACSM data analysis protocols established in previous studies (Ng et al., 2011; Sun et al., 2012), using the standard WaveMetrics Igor Pro-based Data Analysis Software (Version 6.3.5.5) and incorporating calibrations for relative ionization efficiency (RIE), collection efficiency (CE) and detection limit (DL). Further details on data treatment can be found in the Supplement, Sect. 2.

Factors contributing to organic aerosol were explored using PMF (Paatero and Tapper, 1994; Zhang et al., 2011) with the Igor-Pro-based PMF evaluation toolkit (PET) (Ulbrich et al., 2009). In general, PMF can be used to resolve factors as organic aerosol (OA) into hydrocarbon-like OA (HOA), cooking OA (COA), semi-volatile oxygenated OA (SV-OOA), low-volatility oxygenated OA (LV-OOA), and others. The optimal factor number was determined by inter-comparing factors' mass spectra and time series, correlations between factors and related tracers, and correlations with standard mass spectra; solutions with 3, 4, and 5 factors at  $f_{\text{peak}} = 0$  were explored, after which the optimal  $f_{\text{peak}}$  value was determined by repeating the above analysis with varying  $f_{\text{peak}}$  values.

The 4-factor solution (HOA, COA, SV-OOA, LV-OOA) is optimal, with  $Q/Q_{\text{exp}} = 0.8$  and better differentiation between factor time-series ( $R_{\text{pr}} < 0.6$ ; Fig. S4). The factors also correlate well with associated inorganics and external tracers (NO<sub>3</sub>, SO<sub>4</sub>, NH<sub>4</sub>, NO<sub>x</sub>; Zhang et al., 2005, 2011; Ulbrich et al., 2009), e.g. HOA with NO<sub>x</sub>, SV-OOA with NO<sub>3</sub>, LV-OOA with SO<sub>4</sub> and NH<sub>4</sub> (Table S4). Furthermore, the resolved mass spectra of four factors exhibit good similarity (all un-centered  $R$  ( $R_{\text{uc}}$ ) > 0.80) with reference

source mass spectra from the AMS MS database (Ulbrich, I. M., Lechner, M., and Jimenez, J. L., AMS Spectral Database, url: <http://cires.colorado.edu/jimenez-group/AMSsd>; Ulbrich et al., 2009). PMF diagnostic details are shown in the Supplement (Sect. 3) and Fig. S5. We note that  $m/z$  60 and 73 were resolved not only in COA but also in SV-OOA. When PMF was run using only nighttime data (between 00:00 and 06:00 LT), when there is little COA (Fig. S6), these two ions still persist, with similar fractional intensities in SV-OOA as at other times. The time series of  $m/z$  60 and 73 also track well with SV-OOA, with  $R_{pr}$  of 0.92 and 0.93 respectively; hence, we believe that their presence in SV-OOA is not the result of artifacts in PMF.

### 3 Results and discussion

#### 3.1 Mass concentration and chemical composition

Figure 1a and b displays meteorological data (relative humidity, temperature, and precipitation) and mass concentrations of non-refractory  $PM_1$  (NR- $PM_1$ ) species and organic aerosol (OA) components, respectively, between September and December 2013. Total NR- $PM_1$  concentrations vary from 2.1 to 76.4  $\mu\text{g m}^{-3}$  with an average of  $25.9 \pm 13.0 \mu\text{g m}^{-3}$ . ACSM NR- $PM_1$  concentrations co-vary with that of  $PM_{2.5}$  measured by TEOM ( $R^2 = 0.64$ , slope = 0.59; Fig. S1); the low slope value may be caused by the different size cuts of ACSM and TEOM and the presence of refractory materials such as elemental carbon (and to a lesser extent mineral dust and sea salt) which the ACSM cannot detect. Overall, daily  $PM_{2.5}$  concentrations range from 3.7 to 106.0  $\mu\text{g m}^{-3}$  and are largely (90.0 %) within the 24 h air quality standard of 75  $\mu\text{g m}^{-3}$  set by the Hong Kong Air Quality Objectives (HKAQO). Days with better air quality ( $PM_{2.5} < 35 \mu\text{g m}^{-3}$ ) are mainly observed in the month of September and in rainy periods of other months. The prevailing winds from the ocean in September not only bring in less polluted air mass but also dilute the local air pollutants compared with other seasons (Yuan et al.,

[Title Page](#)[Abstract](#)[Introduction](#)[Conclusions](#)[References](#)[Tables](#)[Figures](#)[Back](#)[Close](#)[Full Screen / Esc](#)[Printer-friendly Version](#)[Interactive Discussion](#)

2006; Li et al., 2015). Precipitation has an obvious impact on total NR-PM<sub>1</sub> concentrations, but as we will discuss, has a lesser effect on primary organics.

Overall, NR-PM<sub>1</sub> is dominated by organics and sulfate with relative contributions of 58.2 and 23.3% and average concentrations of  $15.1 \pm 8.1 \mu\text{g m}^{-3}$  and  $6.0 \pm 3.5 \mu\text{g m}^{-3}$ , respectively (Fig. 2a). Other inorganic species (ammonium, nitrate and chloride) amount to approximately 20% of NR-PM<sub>1</sub>. The dominance of organics and sulfate is consistent with previous on-line studies in urban areas (e.g., Salcedo et al., 2006; Aiken et al., 2009; Sun et al., 2012, 2013b) as well as previous filter-based studies in MK (e.g., Louie et al., 2005; Cheng et al., 2010; Huang et al., 2014). The measured composition is consistent with earlier HR-AMS measurements carried out at the same site in spring and summer 2013 (Lee et al., 2015) with very similar overall species distribution, but slightly lower measured concentrations as compared to the ACSM, likely due to the fact that sampling took place in different time periods (spring-summer 2013 for the AMS campaign, fall-winter 2013 for the ACSM campaign). In the AMS study, 6 PMF aerosol factors were identified (one additional OOA factor and one additional COA factor). A marked difference is observed in the distribution of primary OA (POA) and secondary OA (SOA); whereas in spring and summer (AMS), POA makes up 65% of total organics, the reverse is observed for fall and winter (ACSM) where POA only amounts to 42% overall. A possible reason for this discrepancy is the fact that impacts of regional pollution and long-range transport are usually higher during fall and winter (Yuan et al., 2013; Li et al., 2015), thus contributing more SOA.

Elemental carbon (EC) concentrations are significant at the Mong Kok site but not measureable by ACSM due to its high refractory temperature. EC has been discussed extensively in the previously mentioned filter-based studies and a brief comparison of online ECOC measurements to the results of HR-AMS measurements has been presented in an HR-AMS study (Lee et al., 2015). We therefore do not discuss EC in detail in this work.

Continuous measurements at the urban roadside in an ACSM

C. Sun et al.

Title Page

Abstract

Introduction

Conclusions

References

Tables

Figures



Back

Close

Full Screen / Esc

Printer-friendly Version

Interactive Discussion







---

**Continuous measurements at the urban roadside in an ACSM**

---

C. Sun et al.

[Title Page](#)[Abstract](#)[Introduction](#)[Conclusions](#)[References](#)[Tables](#)[Figures](#)[◀](#)[▶](#)[◀](#)[▶](#)[Back](#)[Close](#)[Full Screen / Esc](#)[Printer-friendly Version](#)[Interactive Discussion](#)

19:00–21:00 LT) and non-meal times (00:00–06:00 LT); the non-meal period is defined by the periods of low concentration ( $< 2 \mu\text{g m}^{-3}$ ) in the COA diurnal pattern. During dinner time, the average concentration of organics increases by about  $11 \mu\text{g m}^{-3}$  and its contributions in total NR-PM<sub>1</sub> increase to 70 %, while the concentrations of other species do not change much (Fig. 6b). As shown in Fig. 6c, the increase in organic concentrations results from the increase in COA from  $1.7$  to  $7.8 \mu\text{g m}^{-3}$  ( $\sim 360$  % increase), and to a lesser extent increases in SV-OOA (from  $1.5$  to  $4.5 \mu\text{g m}^{-3}$ , a  $\sim 200$  % increase) and in HOA (from  $1.4$  to  $3.2 \mu\text{g m}^{-3}$ , a  $\sim 130$  % increase). As shown in Table 1, the average concentration of organics during dinner time is  $5 \mu\text{g m}^{-3}$  higher than that during lunch, and this increase is attributed to the increase of COA and SV-OOA mass but not of HOA. This is consistent with the expectation that the cooking activities at MK are higher during dinner than during lunch, while traffic during dinner is comparable to or smaller than that during lunch (Fig. 4f and h). The increase of SV-OOA during dinner time may be the result of enhanced cooking emissions and possibly less evaporation due to lower ambient temperature; contributions from traffic emissions are not likely to be important since there is little increase of HOA during meal time.

### 3.2.3 Oxygenated OA (OOA)

The LV-OOA spectrum correlates well with the standard LV-OOA spectrum (Fig. 3), with a  $R_{\text{uc}}$  of 0.97. The LV-OOA time series is associated with that of  $\text{SO}_4^{2-}$  with a  $R_{\text{pr}}$  of 0.86 (Fig. 1), consistent with reports in the literature (DeCarlo et al., 2010; He et al., 2011; Zhang et al., 2014; Tiitta et al., 2014). The LV-OOA diurnal pattern varies little, suggesting that it is part of the background aerosol, possibly resulting from long range transport (Li et al., 2013, 2015).

The mass spectrum of SV-OOA closely resembles that of “standard” SV-OOA (Fig. 3). Some marker fragments of COA and HOA, for example,  $m/z$  41, 43, 55, and 57, are present in the SV-OOA mass spectrum. SV-OOA concentrations are also weakly associated with those of HOA and their co-emitted precursors (benzene and toluene), with  $R_{\text{pr}}$  of 0.58, 0.65 and 0.51 respectively. In fact, the correlation between





those observed in other periods. Thus, HOA overall has a stronger relationship to SV-OOA than COA has. Cooking emissions reflected by COA are not as important to SV-OOA in the BT periods but they can be important during MT periods. Some SV-OOA might also have converted to LV-OOA under  $\text{HiO}_x$ , although overall most LV-OOA is considered to be from transport.

### 3.3 Diurnal patterns

The diurnal profiles of NR-PM<sub>1</sub> species and OA components are depicted in Fig. 4. Total organics display a diurnal pattern with two pronounced peaks during 12:00–14:00 and 19:00–21:00 LT, corresponding to the peaks of COA at lunch and dinner time respectively. In addition, organics increase at about 10 a.m., which may be related to the increase of local emissions of HOA and COA by 2.3 and 1.1  $\mu\text{g m}^{-3}$  respectively from 06:00 to 10:00 LT.

The mass concentration of sulfate (Fig. 4b) does not show any diel variation. It is likely that sulfate, as a regional pollutant, is mainly formed during long-range transport, leading to the lack of a specific diurnal pattern at MK; a similar flat diurnal pattern for sulfate has also been found at the HKUST supersite in Hong Kong (Lee et al., 2013; Li et al., 2015). These results differ significantly from observations in Beijing and Lanzhou in China and Welgegund in South Africa (Sun et al., 2012, 2013b; Xu et al., 2014; Tiitta et al., 2014) where sulfate displays an obvious increase at noon-time in summer and wet seasons due to either photochemical reaction or aqueous oxidation of  $\text{SO}_2$ . The difference may result from the much lower level of sulfur dioxide ( $\text{SO}_2$ ) with an average of 4.6 ppb in MK compared to for example, ~ 32 ppb in Beijing, where coal combustion leads to a much higher  $\text{SO}_2$  concentration (Lin et al., 2011); sulfate and relative humidity (RH) have almost no correlation ( $R^2 = 0.06$ ) in MK, suggesting that local aqueous processing may not be significant for sulfate observed at Mong Kok.

Nitrate shows a slight dip around noontime, corresponding to the increase of the ambient temperature (Fig. 4j); evaporative loss of particulate nitrate might outweigh the secondary production of nitrate during this time. The diurnal pattern of ammonium

Continuous measurements at the urban roadside in an ACSM

C. Sun et al.

Title Page

Abstract

Introduction

Conclusions

References

Tables

Figures



Back

Close

Full Screen / Esc

Printer-friendly Version

Interactive Discussion



(Fig. 4d) is very similar to that of sulfate, as expected based on their commonly observed association in atmospheric particles. Chloride (Fig. 4e) has rather low concentrations and shows a similar diurnal variation to that of nitrate, likely due to its volatility.

### 3.4 Day-of-week patterns

Figure 8a shows the average concentration trends on individual days of the week for NR-PM<sub>1</sub> species and Fig. 8b describes the diurnal patterns of the OA components for weekdays, Saturdays and Sundays, respectively. Because of the small datasets on Saturdays and Sundays, data beyond one standard deviation from the mean ( $25.9 \pm 13.0 \mu\text{g m}^{-3}$ ) were removed from the whole dataset to remove the influence of episodic events in this analysis. Overall, total NR-PM<sub>1</sub> concentrations have no obvious variation (average variation less than 5%) from Monday to Saturday, but drop by 16% on Sundays compared to Saturdays. This weekend difference is opposite to the result found in Beijing where higher concentrations occur on Sundays than Saturdays (Sun et al., 2013b). On the other hand, some others such as Lough et al. (2006) and Rattigan et al. (2010) reported that both Saturdays and Sundays had obvious traffic emissions reduction due to less human activities on weekends in Los Angeles and New York, respectively.

Organics and secondary inorganics (SO<sub>4</sub>, NH<sub>4</sub> and NO<sub>3</sub>) contributed 54 and 46% respectively to the concentration difference between Sundays and Saturdays in MK. The difference in organics is mainly attributed to the variation of HOA, which shows very similar diurnal variations on Saturdays and weekdays, but has an average decrease of 23% after 07:00 LT on Sundays. A 37% reduction of traffic-related carbonaceous aerosol on Sundays compared with weekdays in MK has been reported (Huang et al., 2014). In Hong Kong many people work on Saturday, which leads to a traffic pattern similar to normal weekdays. COA shows nearly the same diurnal patterns on all days, and LV-OOA and SV-OOA do not show obvious variations. Overall, local emissions from traffic contribute most to the day-of-week variations in organics.

## Continuous measurements at the urban roadside in an ACSM

C. Sun et al.

[Title Page](#)[Abstract](#)[Introduction](#)[Conclusions](#)[References](#)[Tables](#)[Figures](#)[Back](#)[Close](#)[Full Screen / Esc](#)[Printer-friendly Version](#)[Interactive Discussion](#)



high hourly PM levels, LV-OOA/SV-OOA are responsible for episodic events and high day-to-day PM levels.

To analyze the difference in particle composition and meteorological conditions among episodic periods and clean periods, three heavy polluted episodes (19–22, 23–26 October and 10–13 December) and two clean periods (17–18 September and 14–18 December), highlighted in shaded regions in Fig. 1, were analyzed. The average concentrations of these chosen periods are larger than one standard deviation from the average concentration of the campaign ( $25.9 \pm 13.0 \mu\text{g m}^{-3}$ ). The composition, meteorological features ( $T$  and RH) and oxidation index ( $\text{O}_x$  and  $f_{44}$ ) of these five events are shown in Table 4. Clean period 1 (C1) is characterized by low NR-PM<sub>1</sub> concentrations (below  $13 \mu\text{g m}^{-3}$ ), prevailing coastal wind (easterly wind), lack of rain, high ambient temperature ( $\sim 28^\circ\text{C}$ ) and high relative humidity ( $\sim 70\%$ ). Another clean period (C2) features continuous precipitation with the coldest and most humid weather condition in the period studied. Haze period 1 (H1) has similar temperature and humidity as C1 but is marked by mixed continental/oceanic winds. From H1 to the following haze period (H2), the observed wind direction shifts to reflect continental transport, with a significant decrease in RH to 36%. Haze period 3 (H3), just before C2, is also dominated by continental winds but with lower temperatures ( $\sim 19^\circ\text{C}$ ) than during other haze events.

The total NR-PM<sub>1</sub> of C1 ( $12.2 \mu\text{g m}^{-3}$ ) is only 25–30% of that during haze periods and this is mainly attributed to easterly wind bringing less air pollutants and diluting local air pollutants. HOA, COA and SV-OOA in C1 are lower than in C2 despite the lack of rain during C1; their low concentrations during C1 may be influenced by both particle evaporation during high temperatures, especially for SV-OOA, and dilution of local emissions

Compared to the adjacent period H3, precipitation in C2 dramatically reduces the concentration of secondary species such as  $\text{SO}_4$ ,  $\text{NH}_4$ ,  $\text{NO}_3$ , SV-OOA and LV-OOA, but not primary HOA and COA. The total organic mass reduces by 68% to an average of  $8.1 \mu\text{g m}^{-3}$  (Table 4). Precipitation effectively removes secondary particles but is less efficient for primary particles that are continuously generated locally.

Continuous measurements at the urban roadside in an ACSM

C. Sun et al.

Title Page

Abstract

Introduction

Conclusions

References

Tables

Figures



Back

Close

Full Screen / Esc

Printer-friendly Version

Interactive Discussion







**Continuous measurements at the urban roadside in an ACSM**

C. Sun et al.

[Title Page](#)[Abstract](#)[Introduction](#)[Conclusions](#)[References](#)[Tables](#)[Figures](#)[Back](#)[Close](#)[Full Screen / Esc](#)[Printer-friendly Version](#)[Interactive Discussion](#)

The contributions of individual species and OA factors to high NR-PM<sub>1</sub> were analyzed based on hourly data and daily data. It suggests that while cooking is responsible for the hourly high concentrations during meal times, LV-OOA/SV-OOA are responsible for episodic events and high daily PM concentration. Three heavily polluted episodes and two clean periods were recorded during sampling and attributed to different meteorological and circulatory conditions. The analysis of clean periods shows that precipitation has an obvious deposition impact on total NR-PM<sub>1</sub> concentrations, but has a lesser effect on primary organics. Clean ocean wind not only brings in less polluted air mass, but also dilutes the local air pollutants. During this campaign, high-PM events are generally related to continental air mass influence or land-see breeze circulatory conditions, which has less influence on primary emissions but significant effects on secondary particles, with a pronounced increase in the secondary OA contribution during haze events (from 30 to 50 %).

**The Supplement related to this article is available online at doi:10.5194/acpd-15-19405-2015-supplement.**

*Acknowledgements.* The Aerodyne Aerosol Chemical Speciation Monitor measurements were part of the Hong Kong Environmental Protection Department (HKEPD) project ref.: 13-00986. Other data including meteorological data, volatile organic compounds (VOCs) and standard criteria pollutants (NO<sub>x</sub>, SO<sub>2</sub> and PM<sub>2.5</sub>) were kindly provided by the Hong Kong Environmental Protection Department (HKEPD).

Funding support for Berto P. Lee by the Research Grants Council (RGC) of Hong Kong under the Hong Kong PhD Fellowship Scheme (HKPFS) is gratefully acknowledged.

*Disclaimer.* The opinions expressed in this paper are those of the author and do not necessarily reflect the views or policies of the Government of the Hong Kong Special Administrative Region, nor does any mention of trade names or commercial products constitute an endorsement or recommendation of their use.

## References

- Aiken, A. C., DeCarlo, P. F., Kroll, J. H., Worsnop, D. R., Huffman, J. A., Docherty, K. S., Ulbrich, I. M., Mohr, C., Kimmel, J. R., Sueper, D., Sun, Y., Zhang, Q., Trimborn, A., Northway, M., Ziemann, P. J., Canagaratna, M. R., Onasch, T. B., Alfarra, M. R., Prevot, A. S., Dommen, J., Duplissy, J., Metzger, A., Baltensperger, U., and Jimenez, J. L.: O/C and OM/OC ratios of primary, secondary, and ambient organic aerosols with high-resolution time-of-flight aerosol mass spectrometry, *Environ. Sci. Technol.*, 42, 4478–4485, doi:10.1021/es703009q, 2008.
- Aiken, A. C., Salcedo, D., Cubison, M. J., Huffman, J. A., DeCarlo, P. F., Ulbrich, I. M., Docherty, K. S., Sueper, D., Kimmel, J. R., Worsnop, D. R., Trimborn, A., Northway, M., Stone, E. A., Schauer, J. J., Volkamer, R. M., Fortner, E., de Foy, B., Wang, J., Laskin, A., Shutthanandan, V., Zheng, J., Zhang, R., Gaffney, J., Marley, N. A., Paredes-Miranda, G., Arnott, W. P., Molina, L. T., Sosa, G., and Jimenez, J. L.: Mexico City aerosol analysis during MILAGRO using high resolution aerosol mass spectrometry at the urban supersite (T0) – Part 1: Fine particle composition and organic source apportionment, *Atmos. Chem. Phys.*, 9, 6633–6653, doi:10.5194/acp-9-6633-2009, 2009.
- Allan, J. D., Williams, P. I., Morgan, W. T., Martin, C. L., Flynn, M. J., Lee, J., Nemitz, E., Phillips, G. J., Gallagher, M. W., and Coe, H.: Contributions from transport, solid fuel burning and cooking to primary organic aerosols in two UK cities, *Atmos. Chem. Phys.*, 10, 647–668, doi:10.5194/acp-10-647-2010, 2010.
- Bougiatioti, A., Stavroulas, I., Kostenidou, E., Zarrmpas, P., Theodosi, C., Kouvarakis, G., Canonaco, F., Prévôt, A. S. H., Nenes, A., Pandis, S. N., and Mihalopoulos, N.: Processing of biomass-burning aerosol in the eastern Mediterranean during summertime, *Atmos. Chem. Phys.*, 14, 4793–4807, doi:10.5194/acp-14-4793-2014, 2014.
- Budisulistiorini, S. H., Canagaratna, M. R., Croteau, P. L., Marth, W. J., Baumann, K., Edgerton, E. S., Shaw, S. L., Knipping, E. M., Worsnop, D. R., Jayne, J. T., Gold, A., and Surratt, J. D.: Real-time continuous characterization of secondary organic aerosol derived from isoprene epoxydiols in downtown Atlanta, Georgia, using the Aerodyne aerosol chemical speciation monitor, *Environ. Sci. Technol.*, 47, 5686–5694, doi:10.1021/es400023n, 2013.
- Canonaco, F., Crippa, M., Slowik, J. G., Baltensperger, U., and Prévôt, A. S. H.: SoFi, an IGOR-based interface for the efficient use of the generalized multilinear engine (ME-2) for the

### Continuous measurements at the urban roadside in an ACSM

C. Sun et al.

Title Page

Abstract

Introduction

Conclusions

References

Tables

Figures



Back

Close

Full Screen / Esc

Printer-friendly Version

Interactive Discussion





**Continuous  
measurements at the  
urban roadside in an  
ACSM**

C. Sun et al.

Title Page

Abstract

Introduction

Conclusions

References

Tables

Figures



Back

Close

Full Screen / Esc

Printer-friendly Version

Interactive Discussion



Huang, X. H. H., Bian, Q. J., Louie, P. K. K., and Yu, J. Z.: Contributions of vehicular carbonaceous aerosols to PM<sub>2.5</sub> in a roadside environment in Hong Kong, *Atmos. Chem. Phys.*, 14, 9279–9293, doi:10.5194/acp-14-9279-2014, 2014.

Huang, Y., Ho, S. S. H., Ho, K. F., Lee, S. C., Yu, J. Z., and Louie, P. K. K.: Characteristics and health impacts of VOCs and carbonyls associated with residential cooking activities in Hong Kong, *J. Hazard. Mater.*, 186, 344–351, doi:10.1016/j.jhazmat.2010.11.003, 2011.

Jimenez, J. L., Canagaratna, M. R., Donahue, N. M., Prevot, A. S. H., Zhang, Q., Kroll, J. H., DeCarlo, P. F., Allan, J. D., Coe, H., Ng, N. L., Aiken, A. C., Docherty, K. S., Ulbrich, I. M., Grieshop, A. P., Robinson, A. L., Duplissy, J., Smith, J. D., Wilson, K. R., Lanz, V. A., Hueglin, C., Sun, Y. L., Tian, J., Laaksonen, A., Raatikainen, T., Rautiainen, J., Vaattovaara, P., Ehn, M., Kulmala, M., Tomlinson, J. M., Collins, D. R., Cubison, M. J., Dunlea, J., Huffman, J. A., Onasch, T. B., Alfarra, M. R., Williams, P. I., Bower, K., Kondo, Y., Schneider, J., Drewnick, F., Borrmann, S., Weimer, S., Demerjian, K., Salcedo, D., Cottrell, L., Griffin, R., Takami, A., Miyoshi, T., Hatakeyama, S., Shimono, A., Sun, J. Y., Zhang, Y. M., Dzepina, K., Kimmel, J. R., Sueper, D., Jayne, J. T., Herndon, S. C., Trimborn, A. M., Williams, L. R., Wood, E. C., Middlebrook, A. M., Kolb, C. E., Baltensperger, U., and Worsnop, D. R.: Evolution of organic aerosols in the atmosphere, *Science*, 326, 1525–1529, doi:10.1126/science.1180353, 2009.

Laowagul, W., Yoshizumi, K., Mutchimwong, A., Thavipoke, P., Hooper, M., Garivait, H., and Limpaseni, W.: Characterisation of ambient benzene, toluene, ethylbenzene and *m*-, *p*- and *o*-xylene in an urban traffic area in Bangkok, Thailand, *Int. J. Environ. Pollut.*, 36, 241–254, doi:10.1504/ijep.2009.021829, 2009.

Lee, B. P., Li, Y. J., Yu, J. Z., Louie, P. K. K., and Chan, C. K.: Physical and chemical characterization of ambient aerosol by HR-ToF-AMS at a suburban site in Hong Kong during springtime 2011, *J. Geophys. Res.*, 118, 8625–8639, doi:10.1002/jgrd.50658, 2013.

Lee, B. P., Li, Y. J., Yu, J. Z., Louie, P. K. K., and Chan, C. K.: Characteristics of submicron particulate matter at the urban roadside in downtown Hong Kong – overview of 4 months of continuous high-resolution aerosol mass spectrometer (HR-AMS) measurements, *J. Geophys. Res.*, accepted, doi:10.1002/2015JD023311, 2015.

Lee, S. C., Cheng, Y., Ho, K. F., Cao, J. J., Louie, P. K. K., Chow, J. C., and Watson, J. G.: PM<sub>1.0</sub> and PM<sub>2.5</sub> characteristics in the roadside Environment of Hong Kong, *Environ. Sci. Technol.*, 40, 157–165, doi:10.1080/02786820500494544, 2006.

**Continuous  
measurements at the  
urban roadside in an  
ACSM**

C. Sun et al.

Title Page

Abstract

Introduction

Conclusions

References

Tables

Figures

◀

▶

◀

▶

Back

Close

Full Screen / Esc

Printer-friendly Version

Interactive Discussion



Li, Y. J., Lee, B. Y. L., Yu, J. Z., Ng, N. L., and Chan, C. K.: Evaluating the degree of oxygenation of organic aerosol during foggy and hazy days in Hong Kong using high-resolution time-of-flight aerosol mass spectrometry (HR-ToF-AMS), *Atmos. Chem. Phys.*, 13, 8739–8753, doi:10.5194/acp-13-8739-2013, 2013.

5 Li, Y. J., Huang, D. D., Cheung, H. Y., Lee, A. K. Y., and Chan, C. K.: Aqueous-phase photochemical oxidation and direct photolysis of vanillin – a model compound of methoxy phenols from biomass burning, *Atmos. Chem. Phys.*, 14, 2871–2885, doi:10.5194/acp-14-2871-2014, 2014.

10 Li, Y. J., Lee, B. P., Su, L., Fung, J. C. H., and Chan, C.K.: Seasonal characteristics of fine particulate matter (PM) based on high-resolution time-of-flight aerosol mass spectrometric (HR-ToF-AMS) measurements at the HKUST Supersite in Hong Kong, *Atmos. Chem. Phys.*, 15, 37–53, doi:10.5194/acp-15-37-2015, 2015.

15 Lin, W., Xu, X., Ge, B., and Liu, X.: Gaseous pollutants in Beijing urban area during the heating period 2007–2008: variability, sources, meteorological, and chemical impacts, *Atmos. Chem. Phys.*, 11, 8157–8170, doi:10.5194/acp-11-8157-2011, 2011.

Lo, J. C. F., Lau, A. K. H., Fung, J. C. H., and Chen, F.: Investigation of enhanced cross-city transport and trapping of air pollutants by coastal and urban land–sea breeze circulations, *J. Geophys. Res.*, 111, D14104, doi:10.1029/2005jd006837, 2006.

20 Lough, G. C., Schauer, J. J., and Lawson, D. R.: Day-of-week trends in carbonaceous aerosol composition in the urban atmosphere, *Atmos. Environ.*, 40, 4137–4149, doi:10.1016/j.atmosenv.2006.03.009, 2006.

Louie, P. K. K., Chow, J. C., Chen, L. W., Antony, W., John, G., Leung, G., and Sin, D. W. M.: PM<sub>2.5</sub> chemical composition in Hong Kong: urban and regional variations, *Sci. Total Environ.*, 338, 267–281, doi:10.1016/j.scitotenv.2004.07.021, 2005.

25 Minguillón, M. C., Ripoll, A., Pérez, N., Prévôt, A. S. H., Canonaco, F., Querol, X., and Alastuey, A.: Chemical characterization of submicron regional background aerosols in the western Mediterranean using an Aerosol Chemical Speciation Monitor, *Atmos. Chem. Phys.*, 15, 6379–6391, doi:10.5194/acp-15-6379-2015, 2015.

30 Mohr, C., DeCarlo, P. F., Heringa, M. F., Chirico, R., Slowik, J. G., Richter, R., Reche, C., Alastuey, A., Querol, X., Seco, R., Peñuelas, J., Jiménez, J. L., Crippa, M., Zimmermann, R., Baltensperger, U., and Prévôt, A. S. H.: Identification and quantification of organic aerosol from cooking and other sources in Barcelona using aerosol mass spectrometer data, *Atmos. Chem. Phys.*, 12, 1649–1665, doi:10.5194/acp-12-1649-2012, 2012.

**Continuous  
measurements at the  
urban roadside in an  
ACSM**

C. Sun et al.

Title Page

Abstract

Introduction

Conclusions

References

Tables

Figures



Back

Close

Full Screen / Esc

Printer-friendly Version

Interactive Discussion

Ng, N. L., Herndon, S. C., Trimborn, A., Canagaratna, M. R., Croteau, P. L., Onasch, T. B., Sueper, D., Worsnop, D. R., Zhang, Q., Sun, Y. L., and Jayne, J. T.: An Aerosol Chemical Speciation Monitor (ACSM) for routine monitoring of the composition and mass concentrations of ambient aerosol, *Aerosol Sci. Tech.*, 45, 780–794, doi:10.1080/02786826.2011.560211, 2011.

Nie, W., Wang, T., Wang, W., Wei, X., and Liu, Q.: Atmospheric concentrations of particulate sulfate and nitrate in Hong Kong during 1995–2008: impact of local emission and super-regional transport, *Atmos. Environ.*, 76, 43–51, doi:10.1016/j.atmosenv.2012.07.001, 2013.

Paatero, P. and Tapper, U.: Positive matrix factorization: a non-negative factor model with optimal utilization of error estimates of data values, *Environmetrics*, 5, 111–126, doi:10.1002/env.3170050203, 1994.

Petit, J.-E., Favez, O., Sciare, J., Crenn, V., Sarda-Estève, R., Bonnaire, N., Močnik, G., Dupont, J.-C., Haeffelin, M., and Leoz-Garziandia, E.: Two years of near real-time chemical composition of submicron aerosols in the region of Paris using an Aerosol Chemical Speciation Monitor (ACSM) and a multi-wavelength Aethalometer, *Atmos. Chem. Phys.*, 15, 2985–3005, doi:10.5194/acp-15-2985-2015, 2015.

Rattigan, O. V., Dirk Felton, H., Bae, M. S., Schwab, J. J., and Demerjian, K. L.: Multi-year hourly  $PM_{2.5}$  carbon measurements in New York: diurnal, day of week and seasonal patterns, *Atmos. Environ.*, 44, 2043–2053, doi:10.1016/j.atmosenv.2010.01.019, 2010.

Ripoll, A., Minguillón, M. C., Pey, J., Jimenez, J. L., Day, D. A., Sosedova, Y., Canonaco, F., Prévôt, A. S. H., Querol, X., and Alastuey, A.: Long-term real-time chemical characterization of submicron aerosols at Montsec (southern Pyrenees, 1570 m a.s.l.), *Atmos. Chem. Phys.*, 15, 2935–2951, doi:10.5194/acp-15-2935-2015, 2015.

Salcedo, D., Onasch, T. B., Dzepina, K., Canagaratna, M. R., Zhang, Q., Huffman, J. A., DeCarlo, P. F., Jayne, J. T., Mortimer, P., Worsnop, D. R., Kolb, C. E., Johnson, K. S., Zuberi, B., Marr, L. C., Volkamer, R., Molina, L. T., Molina, M. J., Cardenas, B., Bernabé, R. M., Márquez, C., Gaffney, J. S., Marley, N. A., Laskin, A., Shutthanandan, V., Xie, Y., Brune, W., Leshner, R., Shirley, T., and Jimenez, J. L.: Characterization of ambient aerosols in Mexico City during the MCMA-2003 campaign with Aerosol Mass Spectrometry: results from the CENICA Supersite, *Atmos. Chem. Phys.*, 6, 925–946, doi:10.5194/acp-6-925-2006, 2006.

Sun, Y. L., Wang, Z. F., Dong, H. B., Yang, T., Li, J., Pan, X., Chen, P., and Jayne, J. T.: Characterization of summer organic and inorganic aerosols in Beijing, China with an Aerosol Chem-

**Continuous  
measurements at the  
urban roadside in an  
ACSM**

C. Sun et al.

Title Page

Abstract

Introduction

Conclusions

References

Tables

Figures



Back

Close

Full Screen / Esc

Printer-friendly Version

Interactive Discussion

ical Speciation Monitor, Atmos. Environ., 51, 250–259, doi:10.1016/j.atmosenv.2012.01.013, 2012.

Sun, Y. L., Wang, Z. F., Fu, P. Q., Jiang, Q., Yang, T., Li, J., and Ge, X.: The impact of relative humidity on aerosol composition and evolution processes during wintertime in Beijing, China, Atmos. Environ., 77, 927–934, doi:10.1016/j.atmosenv.2013.06.019, 2013a.

Sun, Y. L., Wang, Z. F., Fu, P. Q., Yang, T., Jiang, Q., Dong, H. B., Li, J., and Jia, J. J.: Aerosol composition, sources and processes during wintertime in Beijing, China, Atmos. Chem. Phys., 13, 4577–4592, doi:10.5194/acp-13-4577-2013, 2013b.

Takahama, S., Johnson, A., Guzman Morales, J., Russell, L. M., Duran, R., Rodriguez, G., Zheng, J., Zhang, R., Toom-Sauntry, D., and Leitch, W. R.: Submicron organic aerosol in Tijuana, Mexico, from local and Southern California sources during the CalMex campaign, Atmos. Environ., 70, 500–512, doi:10.1016/j.atmosenv.2012.07.057, 2013.

Tiitta, P., Vakkari, V., Croteau, P., Beukes, J. P., van Zyl, P. G., Josipovic, M., Venter, A. D., Jaars, K., Pienaar, J. J., Ng, N. L., Canagaratna, M. R., Jayne, J. T., Kerminen, V.-M., Kokkola, H., Kulmala, M., Laaksonen, A., Worsnop, D. R., and Laakso, L.: Chemical composition, main sources and temporal variability of PM<sub>1</sub> aerosols in southern African grassland, Atmos. Chem. Phys., 14, 1909–1927, doi:10.5194/acp-14-1909-2014, 2014.

Ulbrich, I. M., Canagaratna, M. R., Zhang, Q., Worsnop, D. R., and Jimenez, J. L.: Interpretation of organic components from Positive Matrix Factorization of aerosol mass spectrometric data, Atmos. Chem. Phys., 9, 2891–2918, doi:10.5194/acp-9-2891-2009, 2009.

Wanna, L., Hathairatana, G., Wongpun, L., and Kunio, Y.: Ambient Air Concentrations of Benzene, Toluene, Ethylbenzene and Xylene in Bangkok, Thailand during April–August in 2007, Asian J. Atmos. Environ., 2, 14–25, doi:10.5572/ajae.2008.2.1.014, 2008.

Wong, T. W., Tam, W. W. S., Yu, I. T. S., Lau, A. K. H., Pang, S. W., and Wong, A. H. S.: Developing a risk-based air quality health index, Atmos. Environ., 76, 52–58, doi:10.1016/j.atmosenv.2012.06.071, 2013.

Xu, J., Zhang, Q., Chen, M., Ge, X., Ren, J., and Qin, D.: Chemical composition, sources, and processes of urban aerosols during summertime in northwest China: insights from high-resolution aerosol mass spectrometry, Atmos. Chem. Phys., 14, 12593–12611, doi:10.5194/acp-14-12593-2014, 2014.

Yuan, Z. B., Yu, J. Z., Lau, A. K. H., Louie, P. K. K., and Fung, J. C. H.: Application of positive matrix factorization in estimating aerosol secondary organic carbon in Hong Kong and its

relationship with secondary sulfate, *Atmos. Chem. Phys.*, 6, 25–34, doi:10.5194/acp-6-25-2006, 2006.

Yuan, Z. B., Yadav, V., Turner, J. R., Louie, P. K. K., and Lau, A. K. H.: Long-term trends of ambient particulate matter emission source contributions and the accountability of control strategies in Hong Kong over 1998–2008, *Atmos. Environ.*, 76, 21–31, doi:10.1016/j.atmosenv.2012.09.026, 2013.

Zhang, Q., Alfara, M. R., Worsnop, D. R., Allan, J. D., Coe, H., Canagaratna, M. R., and Jimenez, J. L.: Deconvolution and quantification of hydrocarbon-like and oxygenated organic aerosols based on aerosol mass spectrometry, *Environ. Sci. Technol.*, 39, 4938–4952, doi:10.1021/es048568l, 2005.

Zhang, Q., Jimenez, J. L., Canagaratna, M. R., Ulbrich, I. M., Ng, N. L., Worsnop, D. R., and Sun, Y.: Understanding atmospheric organic aerosols via factor analysis of aerosol mass spectrometry: a review, *Anal. Bioanal. Chem.*, 401, 3045–3067, doi:10.1007/s00216-011-5355-y, 2011.

Zhang, Y. J., Tang, L. L., Wang, Z., Yu, H. X., Sun, Y. L., Liu, D., Qin, W., Canonaco, F., Prévôt, A. S. H., Zhang, H. L., and Zhou, H. C.: Insights into characteristics, sources, and evolution of submicron aerosols during harvest seasons in the Yangtze River delta region, China, *Atmos. Chem. Phys.*, 15, 1331–1349, doi:10.5194/acp-15-1331-2015, 2015.

Zhang, Y. M., Zhang, X. Y., Sun, J. Y., Hu, G. Y., Shen, X. J., Wang, Y. Q., Wang, T. T., Wang, D. Z., and Zhao, Y.: Chemical composition and mass size distribution of PM<sub>1</sub> at an elevated site in central east China, *Atmos. Chem. Phys.*, 14, 12237–12249, doi:10.5194/acp-14-12237-2014, 2014.

**Continuous measurements at the urban roadside in an ACSM**

C. Sun et al.

Title Page

Abstract

Introduction

Conclusions

References

Tables

Figures

◀

▶

◀

▶

Back

Close

Full Screen / Esc

Printer-friendly Version

Interactive Discussion



## Continuous measurements at the urban roadside in an ACSM

C. Sun et al.

Title Page

Abstract

Introduction

Conclusions

References

Tables

Figures

◀

▶

◀

▶

Back

Close

Full Screen / Esc

Printer-friendly Version

Interactive Discussion



**Table 1.** Average concentrations of NR-PM<sub>1</sub> and OA components during lunch time, dinner time and non-meal times.

Species $\mu\text{g m}^{-3}$	Lunch	Dinner	Non-meal
Org	18.8	23.7	10.3
SO <sub>4</sub>	5.8	6.1	6.3
NH <sub>4</sub>	2.6	2.9	3.0
NO <sub>3</sub>	1.4	1.8	1.6
Chl	0.1	0.2	0.2
Organic aerosol components			
HOA	3.2	3.2	1.4
COA	6.2	9.6	1.7
LV-OOA	5.8	5.4	5.6
SV-OOA	3.6	5.5	1.5

## Continuous measurements at the urban roadside in an ACSM

C. Sun et al.

[Title Page](#)
[Abstract](#)
[Introduction](#)
[Conclusions](#)
[References](#)
[Tables](#)
[Figures](#)
[◀](#)
[▶](#)
[◀](#)
[▶](#)
[Back](#)
[Close](#)
[Full Screen / Esc](#)
[Printer-friendly Version](#)
[Interactive Discussion](#)


**Table 2.** Regression of SV-OOA on HOA, COA and LV-OOA and concentrations of OA factors and  $O_x$  under high and low temperature (LT and HT) of the three chosen periods (MT, BT and OT).

Period Temperature	Meal time (MT)		Background time (BT)		Other time (OT)	
	LTemp	HTemp	LTemp	HTemp	LTemp	HTemp
	Coefficients <sup>a</sup>					
HOA	0.80	0.56	0.70	0.43	0.48	0.23
COA	0.29	0.15	0.22	0.00	0.31	0.11
LV-OOA	0.25	0.23	0.23	0.24	0.25	0.28
Adjusted $R^2$	0.90	0.81	0.83	0.57	0.85	0.73
	Average Concentration ( $\mu\text{g m}^{-3}$ , ppb)					
HOA	3.71	2.85	1.60	1.18	3.51	2.88
COA	7.34	7.40	1.61	1.54	3.50	3.74
LV-OOA	5.46	5.57	5.91	5.07	5.85	5.99
SV-OOA	6.30	3.89	2.68	1.44	4.1	2.39
$O_x$ (ppb)	83.12	85.23	58.71	53.45	75.06	76.77

<sup>a</sup> The coefficient of HOA, COA and LV-OOA in the regression equation reconstructing SV-OOA under LTemp ( $T < 22.5^\circ\text{C}$ ) and HTemp ( $T > 22.5^\circ\text{C}$ ) during meal time (12:00–14:00, 19:00–21:00 LT), background time (00:00–06:00 LT) and other time. The average temperature of the whole campaign is  $22.5^\circ\text{C}$ . All entries of coefficients are significant at the 1% level (two-tailed), except that of HOA/OT, which is significant at the 5% level.

## Continuous measurements at the urban roadside in an ACSM

C. Sun et al.

[Title Page](#)
[Abstract](#)
[Introduction](#)
[Conclusions](#)
[References](#)
[Tables](#)
[Figures](#)
[◀](#)
[▶](#)
[◀](#)
[▶](#)
[Back](#)
[Close](#)
[Full Screen / Esc](#)
[Printer-friendly Version](#)
[Interactive Discussion](#)


**Table 3.** Regression of SV-OOA on HOA, COA and LV-OOA and concentrations of OA factors and Temperature under high and low  $O_x$  ( $HiO_x$  and  $LO_x$ ) of three chosen periods (MT, BT and OT).

	Meal time (MT)		Background time (BT)		Other time (OT)	
	$LO_x$	$HiO_x$	$LO_x$	$HiO_x$	$LO_x$	$HiO_x$
	Coefficients <sup>a</sup>					
HOA	0.50	1.13	0.62	0.64 <sup>b</sup>	0.08 <sup>b</sup>	0.52
COA	0.13	0.14	0.00	0.15	0.14	0.14
LV-OOA	0.33	0.10 <sup>b</sup>	0.26	0.18	0.34	0.21
Adjusted $R^2$	0.73	0.86	0.73	0.80	0.67	0.78
	Average Concentration ( $\mu\text{g m}^{-3}$ , ppb)					
HOA	2.24	3.41	1.20	2.03	2.11	3.55
COA	7.31	7.57	1.59	1.73	2.77	3.71
LV-OOA	3.50	5.92	5.07	7.22	4.06	6.77
SV-OOA	3.22	5.29	1.85	2.79	1.8	3.56
Temp ( $^{\circ}\text{C}$ )	23.30	23.80	21.48	20.39	22.01	22.74

<sup>a</sup> The coefficient of HOA, COA and LV-OOA in the regression equation reconstructing SV-OOA under  $LO_x$  ( $O_x < 70$  ppb) and  $HiO_x$  ( $O_x > 70$  ppb) during meal time (12:00–14:00, 19:00–21:00 LT), background time (00:00–06:00 LT) and other time. 70 ppb is the average  $O_x$  of the whole study. All entries of coefficients are significant at 1 % level (two-level), except those indicated with <sup>b</sup>, which indicates significance at the 5 % level.



## Continuous measurements at the urban roadside in an ACSM

C. Sun et al.

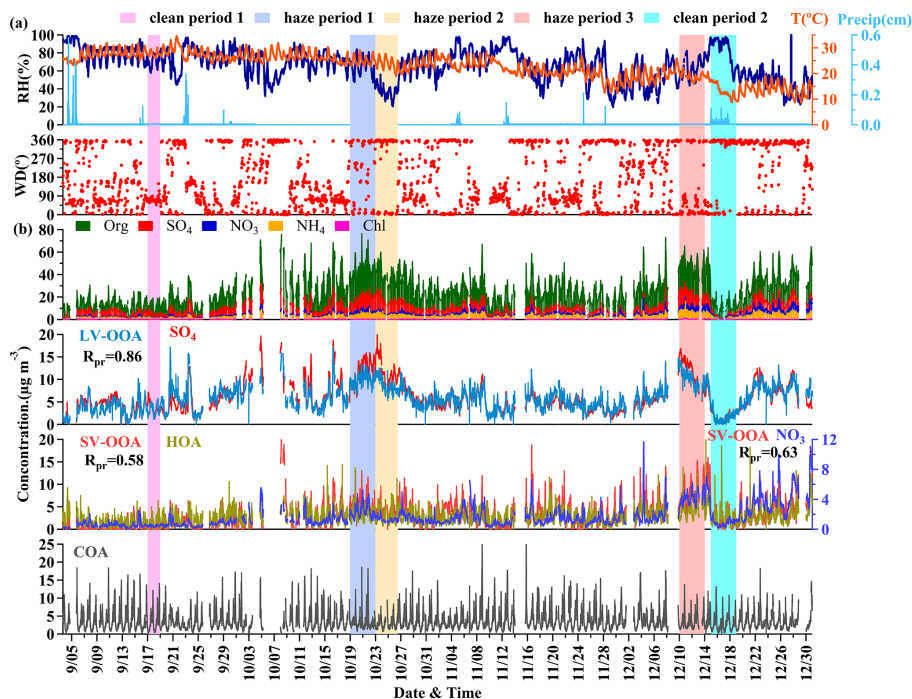


**Figure 1.** Overview of temporal variation of (a) meteorological factors (Relative Humidity, Temperature and Precipitation) and (b) non-refractory PM<sub>1</sub> species (Org, SO<sub>4</sub>, NO<sub>3</sub>, NH<sub>4</sub> and Chl) and organic aerosol components (LV-OOA, SV-OOA, HOA and COA). Five periods: clean period 1 (C1), haze period 1 (H1), haze period 2 (H2), haze period 3 (H3) and clean period 2 (C2) are highlighted.

## Continuous measurements at the urban roadside in an ACSM

C. Sun et al.

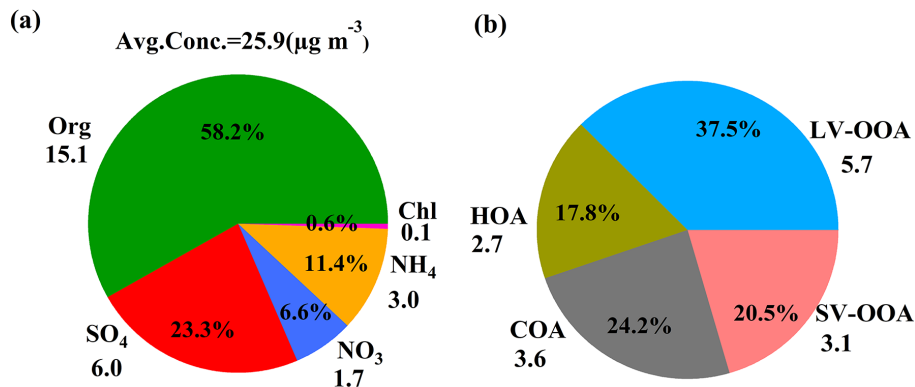


**Figure 2.** Average concentration of each chemical composition of (a) NR-PM<sub>1</sub> (Org, SO<sub>4</sub>, NO<sub>3</sub>, NH<sub>4</sub> and Chl) and (b) organic aerosol (LV-OOA, SV-OOA, HOA and COA).

[Title Page](#)
[Abstract](#)
[Introduction](#)
[Conclusions](#)
[References](#)
[Tables](#)
[Figures](#)
[◀](#)
[▶](#)
[◀](#)
[▶](#)
[Back](#)
[Close](#)
[Full Screen / Esc](#)
[Printer-friendly Version](#)
[Interactive Discussion](#)


## Continuous measurements at the urban roadside in an ACSM

C. Sun et al.

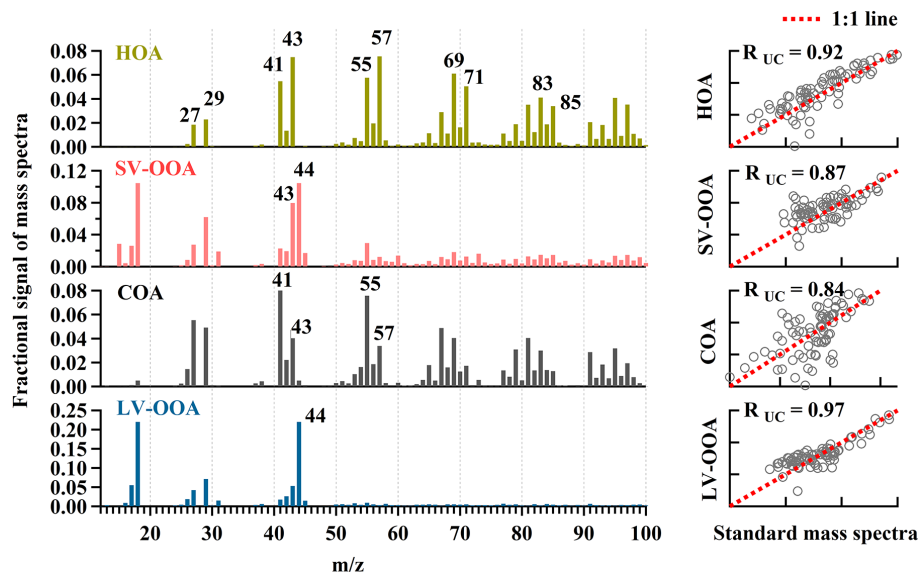


**Figure 3.** Mass spectra of resolved OA components (HOA, SV-OOA, LV-OOA, COA) and the correlation with standard mass spectral profiles available on the AMS MS database (Ulbrich, I. M., Lechner, M., and Jimenez, J. L., AMS Spectral Database). The x and y axes in the right-hand graphs are mass spectra of resolved factor and the standard, respectively.

## Continuous measurements at the urban roadside in an ACSM

C. Sun et al.

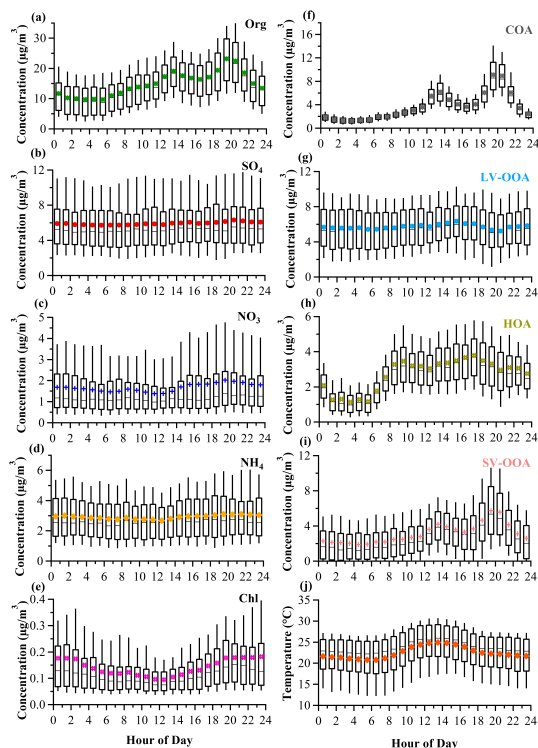


**Figure 4.** Diurnal profiles of NR-PM<sub>1</sub> species, OA components and Temperature for the entire study with 25 and 75 percentile boxes, 10 and 90 percentile whiskers, mean as colored marker and median as black line in the whisker box.

Title Page

Abstract

Introduction

Conclusions

References

Tables

Figures

◀

▶

◀

▶

Back

Close

Full Screen / Esc

Printer-friendly Version

Interactive Discussion



## Continuous measurements at the urban roadside in an ACSM

C. Sun et al.

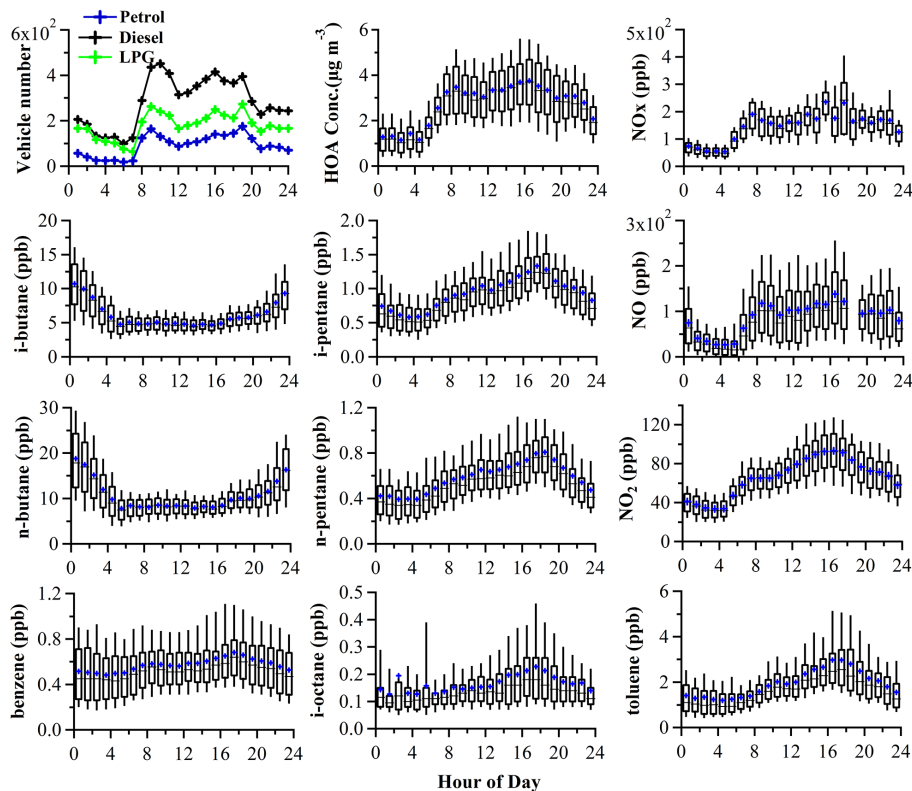


**Figure 5.** Diurnal patterns of vehicle numbers at the Mong Kok site in 28–31 May 2013 and concentrations of HOA,  $\text{NO}_x$ ,  $\text{NO}_2$ , NO, i-pentane, n-pentane, i-octane, i-butane, n-butane, benzene and toluene during the whole study.

[Title Page](#)
[Abstract](#)
[Introduction](#)
[Conclusions](#)
[References](#)
[Tables](#)
[Figures](#)
[Back](#)
[Close](#)
[Full Screen / Esc](#)
[Printer-friendly Version](#)
[Interactive Discussion](#)

## Continuous measurements at the urban roadside in an ACSM

C. Sun et al.

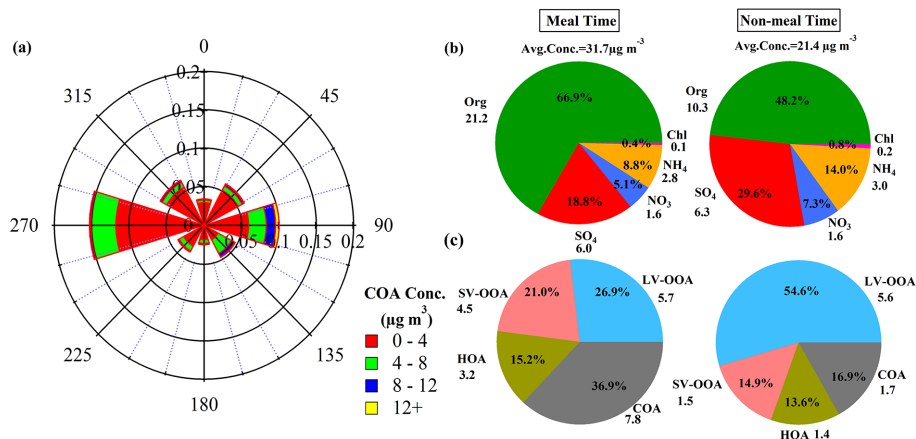


**Figure 6.** (a) Wind rose plot of COA concentration. The angle and radius present the wind direction and its probability, respectively, while color indicates COA concentration. (b) The fractional composition of NR-PM<sub>1</sub> species during meal time (12:00–02:00, 19:00–21:00 LT) and non-meal time (00:00–06:00 LT). (c) The fractional composition of OA during meal time and non-meal time, respectively.

## Continuous measurements at the urban roadside in an ACSM

C. Sun et al.

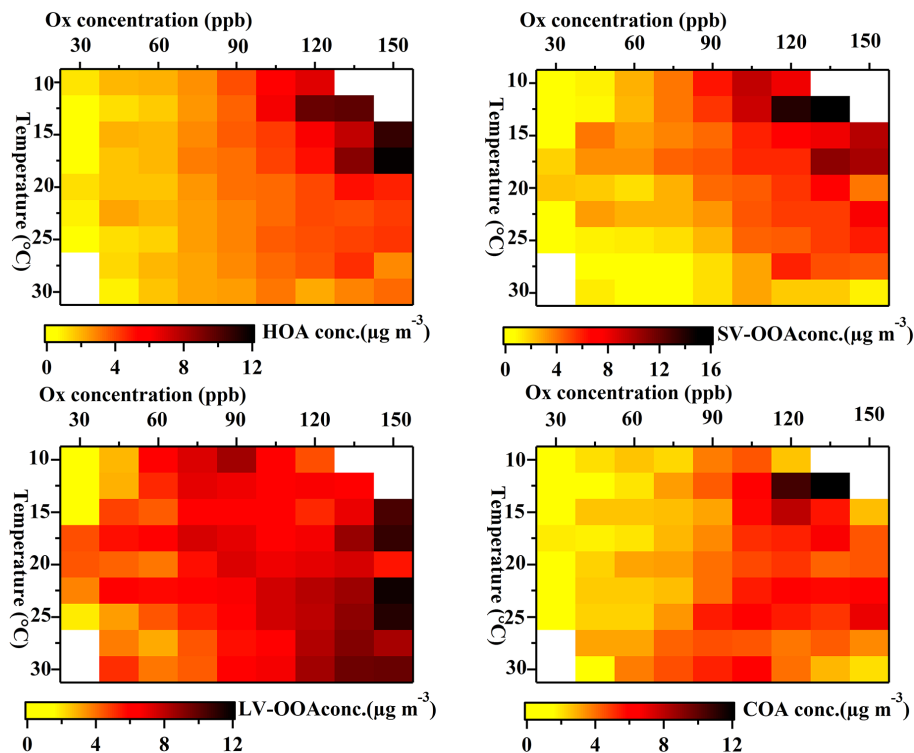


**Figure 7.** Variation of the average concentration of OA components (HOA, SV-OOA, LV-OOA and COA) coded by color as a function of binned  $O_x$  concentration (ppb) and binned temperature ( $^{\circ}C$ ).

[Title Page](#)
[Abstract](#)
[Introduction](#)
[Conclusions](#)
[References](#)
[Tables](#)
[Figures](#)
[◀](#)
[▶](#)
[◀](#)
[▶](#)
[Back](#)
[Close](#)
[Full Screen / Esc](#)
[Printer-friendly Version](#)
[Interactive Discussion](#)


## Continuous measurements at the urban roadside in an ACSM

C. Sun et al.

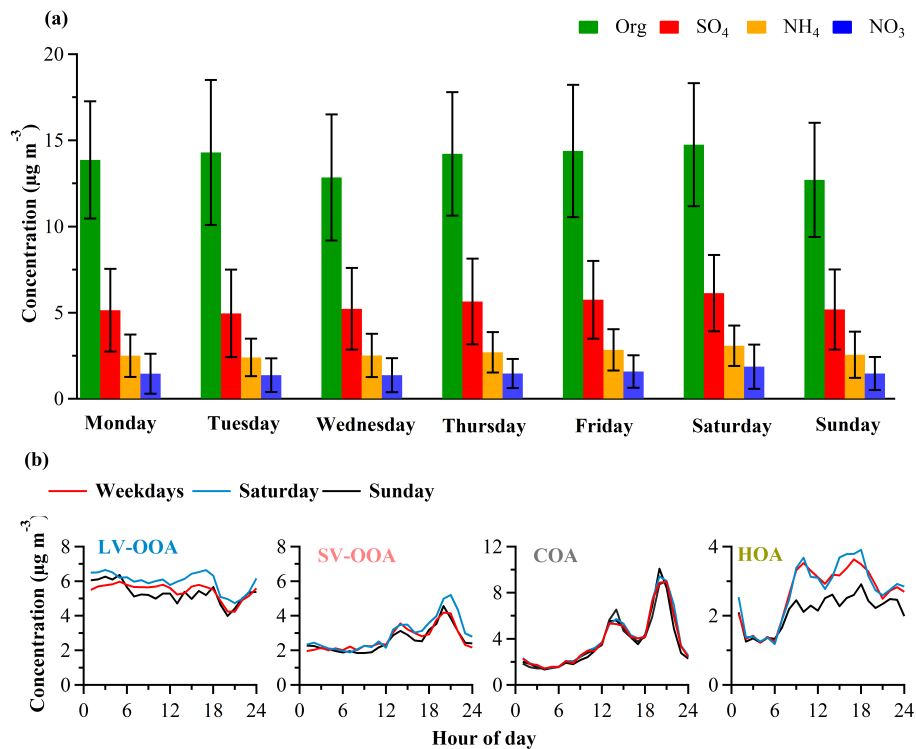


**Figure 8.** (a) Day-of-week variations of NR-PM<sub>1</sub> species (standard deviation as vertical line) and (b) average diurnal patterns of OA components for weekdays, Saturdays and Sundays.

## Continuous measurements at the urban roadside in an ACSM

C. Sun et al.

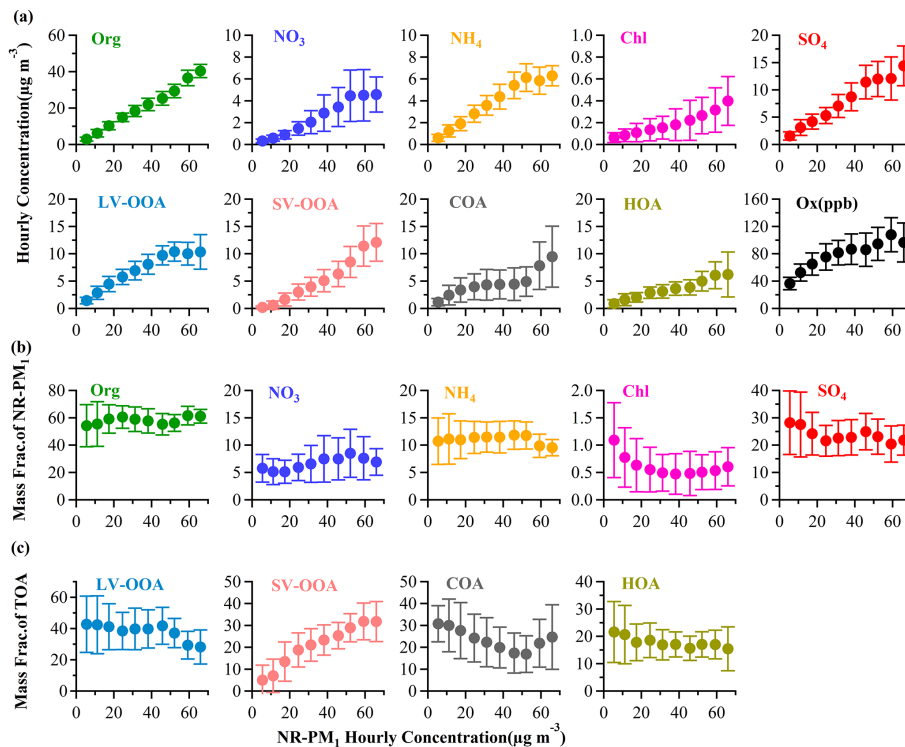


**Figure 9.** (a) Variation in mass concentration of NR-PM<sub>1</sub> species and OA components as a function of total NR-PM<sub>1</sub> mass loading, and (b) mass fraction of total NR-PM<sub>1</sub> for NR-PM<sub>1</sub> species, and (c) mass fraction of total organics for OA components, as a function of total NR-PM<sub>1</sub> mass loading. The data were binned by the hourly average NR-PM<sub>1</sub> mass with a range of 7 μg m<sup>-3</sup>, and the vertical lines are the standard deviation.

[Title Page](#)
[Abstract](#)
[Introduction](#)
[Conclusions](#)
[References](#)
[Tables](#)
[Figures](#)
[Back](#)
[Close](#)
[Full Screen / Esc](#)
[Printer-friendly Version](#)
[Interactive Discussion](#)

## Continuous measurements at the urban roadside in an ACSM

C. Sun et al.

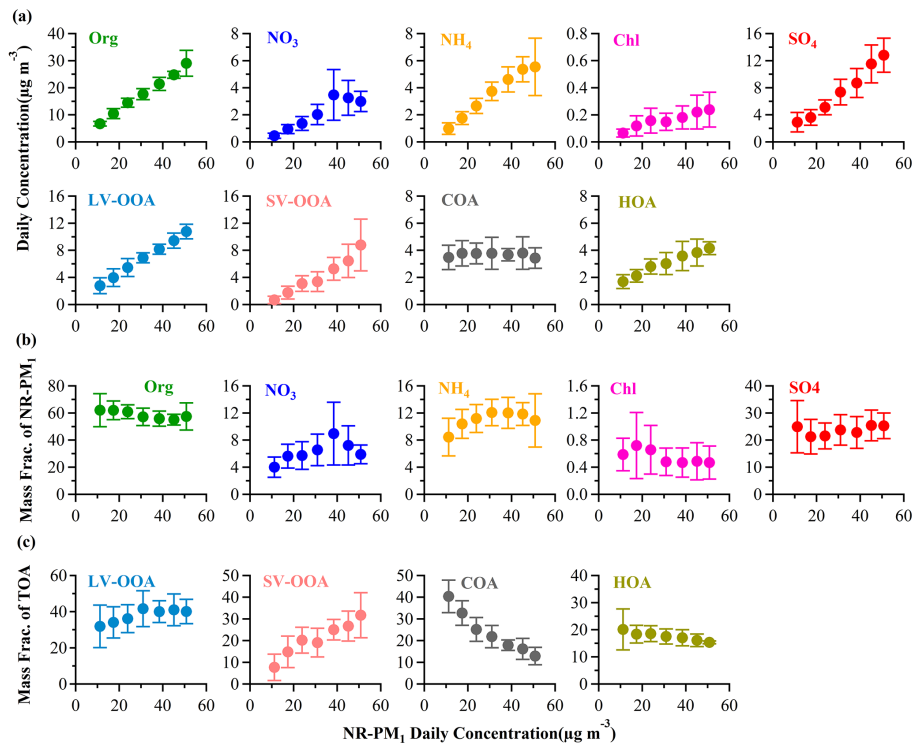


**Figure 10.** (a) Variation in mass concentration of NR-PM<sub>1</sub> species and OA components as a function of total NR-PM<sub>1</sub> mass loading, and (b) mass fraction of total NR-PM<sub>1</sub> for NR-PM<sub>1</sub> species, and (c) mass fraction of total organics for OA components, as a function of total NR-PM<sub>1</sub> mass loading. The data were binned by the *daily average* NR-PM<sub>1</sub> mass with a range of 7 μg m<sup>-3</sup>, and the vertical lines are the standard deviation.

## Continuous measurements at the urban roadside in an ACSM

C. Sun et al.

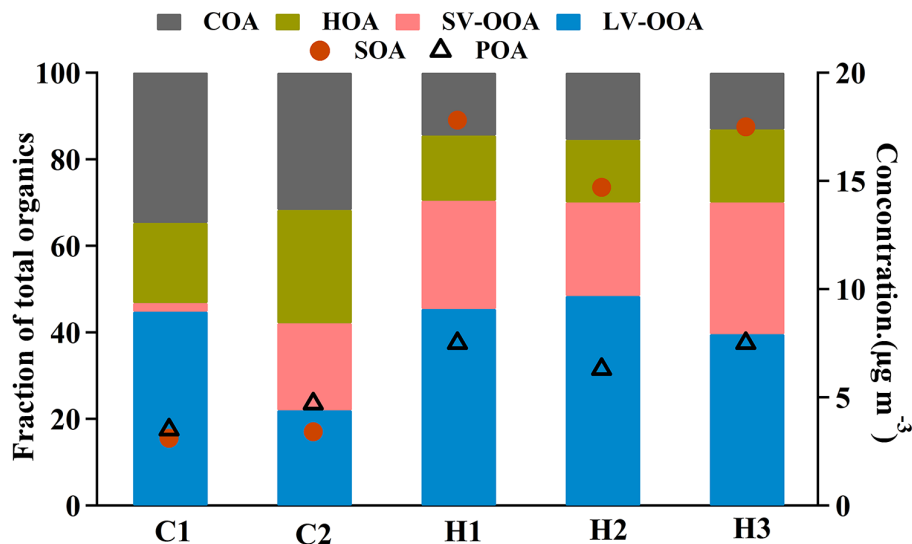


**Figure 11.** Mass fraction of hydrocarbon-like organic aerosol (HOA), cooking organic aerosol (COA), semi-volatile oxygenated organic aerosol (SV-OOA) and low-volatility oxygenated organic aerosol (LV-OOA) in color, and the mass concentration of POA and SOA marked by triangles and circles, respectively, during five periods: clean periods (C1 and C2), and haze periods (H1, H2 and H3).

Title Page

Abstract

Introduction

Conclusions

References

Tables

Figures

◀

▶

◀

▶

Back

Close

Full Screen / Esc

Printer-friendly Version

Interactive Discussion

